CHIN. PHYS. LETT. Vol. 37, No. 3 (2020) 034202

High-Efficiency Broadband Near-Infrared Single-Photon Frequency Upconversion and Detection *

Jian-Hui Ma(马建辉)[1], Hui-Qin Hu(胡慧琴)[1], Yu Chen(陈昱)[1], Guang-Jian Xu(许广建)[1], Hai-Feng Pan(潘海峰)[1], E Wu(武愕)[1,2]**

[1]*State Key Laboratory of Precision Spectroscopy, East China Normal University, Shanghai 200062*
[2]*Collaborative Innovation Center of Extreme Optics, Shanxi University, Taiyuan 030006*

(Received 13 December 2019)

We propose and demonstrate a high efficiency broadband near infrared single-photon upconversion and detection with a broadband pump laser based on sum frequency conversion in the PPLN crystal. By using a pump laser centered at 1040 nm with a spectral bandwidth of 10 nm, the signal single-photons centered at 1562 nm with a broadband bandwidth up to 7.2 nm are frequency-converted from the near infrared to the visible regime. A maximum conversion efficiency of 18.8% is achieved, while the background noise is measured to be only 1.2×10^{-3} *counts/pulse. The corresponding spectral linewidth of the upconverted photons is 0.2 nm. This scheme of broadband infrared single-photon upconversion and detection provides potential solutions in infrared laser ranging, broadband infrared imaging and quantum key distribution.*

PACS: 42.65.−k, 42.65.Ky, 42.62.Fi DOI: 10.1088/0256-307X/37/3/034202

Since the experiment of quantum cryptography was first performed in 1992,[1,2] quantum communication and information processing have been developing rapidly. Furthermore, single photons have consistently played an indispensable role in modern quantum networks.[3−8] Infrared single photons are exploited as carriers for transmitting quantum information between nodes in a quantum network because of the distinctive low loss propagating in fibers and atmosphere.[9−11] However, single photons in quantum storage are usually used at visible wavelengths,[12,13] therefore systems for different applications are spectrally incompatible. The single-photon frequency conversion in nonlinear medium technique bridges photons in infrared wavelength and visible range, and provides solutions for quantum interfaces between different quantum systems.[14−17]

The technique of single-photon frequency upconversion is based on the sum frequency generation (SFG) process, where the signal and converted photons share exactly the same quantum characteristics except for the wavelength.[18,19] Periodically poled lithium niobate (PPLN) crystals are commonly used in frequency upconversion because they have large second-order nonlinear coefficient compared with other nonlinear optical devices.[20,21] For a general sum frequency generation process, the bandwidth of the signal is severely restricted due to the limited PPLN spectral acceptance when using a single line pump. However, the development of quantum communication and information processing applications have created a demand for broadband single-photon frequency upconversion. For example, the bandwidths of quantum memories should match with those of the quantum state carriers and also the sources, while the common spontaneous parametric downconversion sources typically yield spectral bandwidth of up to 300 GHz.[22]

Many solutions have been proposed to break through this problem and achieve broadband infrared single-photon detection.[23−29] Temperature gradient controlled nonlinear medium was applied in frequency upconversion experiment to increase the tolerant signal bandwidth for quasi-phase matching (QPM),[23,24] the SFG bandwidth up to 2.8 nm at 600 nm was achieved in temperature controlled MgO-doped PPLN crystals. Nonlinear crystals with all kinds of grating structures have also been applied for broadband frequency conversion. It has been reported that using an aperiodic poled potassium titanyl phosphate (KTP) device, frequency conversion over a bandwidth of 140 nm was achieved in communication wavelength.[25] Broadband upconversion of light in mid-infrared region through SFG by use of a linearly chirped aperiodic poled ZnO:$LiNbO_3$ waveguide has also been demonstrated.[26] In addition, there is wide spectral bandwidth of phase matching at the tracing point of nonlinear crystals, which has been applied in second harmonic generation and sum frequency generation.[27,28] However, due to the limit of group-velocity mismatch, the phase matching at the tracing point can be only achieved around one specific wavelength, which depends on the properties of nonlinear crystals.

Regardless of angle tuning or temperature tuning, these tuning mechanisms cannot achieve simultaneous phase matching over the entire frequency range for broadband signals. Aperiodic poled PPLN crystals have a strict requirement for the processing technology of crystals. Therefore, a broadband near-infrared pho-

*Supported by the National Natural Science Foundation of China under Grant Nos. 11722431, 11674099 and 11621404, and the Program of Introducing Talents of Discipline to Universities under Grant No. B12024.
**Corresponding author. Email: ewu@phy.ecnu.edu.cn
© 2020 Chinese Physical Society and IOP Publishing Ltd

ton upconversion scheme based on broadband pumping is proposed here, the related theoretical analysis is performed and experimental verification is carried out.

In this Letter, we have achieved infrared signal frequency upconversion at single-photon level by a broadband pumping based on the type-0 quasi-phase matching in a bulk PPLN crystal. Using a strong pump centered at 1040 nm with a broadband spectrum up to 10 nm, and accurately controlling the temperature of nonlinear medium to satisfy phase-matching, a maximum detection efficiency of 18.8% is achieved with a background noise about 1.2×10^{-3} counts/pulse for the infrared single-photon signal centered at 1562 nm with a 7.2 nm bandwidth. The bandwidth of the converted photons is 0.2 nm, corresponding to a spectral compression ratio of 36 via frequency upconversion.

In the process of SFG, conservation of energy and momentum are strictly required. The condition of conservation of energy is satisfied by

$$\hbar\frac{c}{\lambda_{\rm SFG}} = \hbar\frac{c}{\lambda_{\rm s}} + \hbar\frac{c}{\lambda_{\rm p}}, \tag{1}$$

where $\hbar$ is the reduced Planck constant, c is velocity of light, $\lambda_{\rm SFG}$, $\lambda_{\rm s}$ and $\lambda_{\rm p}$ are the wavelengths of the SFG, signal and pump in vacuum, respectively.

Conservation of momentum is achieved by the quasi-phase matching technique when the PPLN is used as the nonlinear medium. The mismatch between interacting waves influences conversion efficiency of the signal to a large extent, and is expressed as[30]

$$\Delta k = 2\pi\left(\frac{n_{\rm SFG}}{\lambda_{\rm SFG}} - \frac{n_{\rm s}}{\lambda_{\rm s}} - \frac{n_{\rm p}}{\lambda_{\rm p}} - \frac{1}{\Lambda}\right), \tag{2}$$

where $n_{\rm SFG}$, $n_{\rm s}$ and $n_{\rm p}$ are the refractive indices of the SFG, signal and pump in the PPLN crystal, respectively, and Λ is the poling period of the PPLN crystal. Equation (2) applies the plane wave approximation.

The normalized photon conversion efficiency can be expressed as

$$\eta(\lambda_{\rm s}) = {\rm sinc}^2\left(\frac{\Delta kL}{2}\right), \tag{3}$$

where L is the PPLN length. Under the condition of $\Delta k = 0$, the conversion efficiency of single photon will reach the theoretical maximum of 100%.

According to Eqs. (1) and (2), when $\Delta k = 0$, we have obtained the function of signal wavelength on pump wavelength as

$$\lambda_{\rm s} = \frac{(n_{\rm SFG} - n_{\rm s})\,\Lambda}{(n_{\rm p} - n_{\rm SFG})\Lambda + \lambda_{\rm p}}\lambda_{\rm p}, \tag{4}$$

then the bandwidth of signal photons which can be upconverted is dependent on the bandwidth of the pump light as

$$\Delta\lambda_{\rm s} = \frac{|n_{\rm SFG} - n_{\rm p}|\,\lambda_{\rm s}^2}{|n_{\rm SFG} - n_{\rm s}|\,\lambda_{\rm p}^2}\Delta\lambda_{\rm p}. \tag{5}$$

Obviously, Eq. (5) indicates that at a given pump laser central wavelength, a wider signal band can be converted when the bandwidth of the pump is wider. In the process of calculation, we have considered the refractive index of interacting waves as constant to simplify the operation process. However, due to the existence of dispersion in the propagation process in the PPLN crystal for broadband signal and pump, the refractive indices of each wave change at different wavelengths, which may lead to deviations for the simulation results.

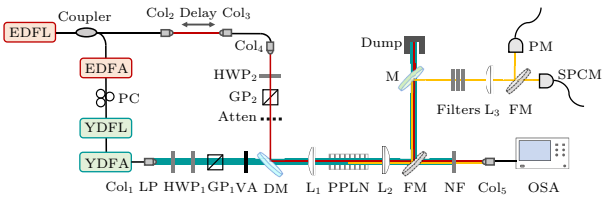

Fig. 1. Schematic of the experimental setup. EDFL: Er-doped fiber laser, YDFL: Yb-doped fiber laser, EDFA: Er-doped fiber amplifier, YDFA: Yb-doped fiber amplifier, PC: polarization controller, $\rm Col_{1,2,3,4,5}$: collimators, LP: long-pass filter cutting off at 1000 nm, $\rm HWP_{1,2}$: half wave plates, $\rm GP_{1,2}$: Glan prisms, VA: variable attenuator, Atten: fixed attenuator, DM: dichroic mirror, $L_{1,2,3}$: lenses, FM: flip mirror, PPLN: periodically poled lithium niobate, M: mirror with high reflectivity at 622 ± 10 nm, NF: notch filter, OSA: optical spectrum analyzer, SPCM: single-photon counting module, PM: power meter.

We built a synchronously pumped SFG system to achieve broadband infrared single-photon frequency upconversion and detection. The scheme of the experimental setup is illustrated in Fig. 1. The setup consisted of the laser sources part, the frequency conversion part and the detection part. The signal and the pump sources were composed of two master-slave synchronized fiber lasers. The signal beam was produced by an Er-doped fiber laser (EDFL) based on nonlinear polarization rotation (NPR) mode locking with a repetition rate of 20.2 MHz. The spectrum of the EDFL output beam was centered at 1562.2 nm with a 9.1 nm full width at half maximum (FWHM) measured by an optical spectrum analyzer (Yokogawa AQ6370), as shown in Fig. 2(a), and the pulse duration was measured to be 0.8 ps. The output beam was separated into two beams by a 1:9 coupler. The weak beam was used as the signal of frequency upconversion system. The other beam was amplified by an Er-doped fiber amplification and then injected into an Yb-doped fiber laser (YDFL) to realize a master-slave synchronization in repetition rate between the two lasers. The YDFL was constructed based on NPR mode locking in a full positive dispersion cavity. After being amplified by an Yb-doped fiber amplifier (YDFA), the average power of the output reached 65 mW which fulfilled the requirements of the strong pump in frequency upconversion process. The spectrum of the pump beam centered at 1040 nm with the FWHM of 10 nm as shown in Fig. 2(b). The pulse duration of the pump beam was engineered to be 22.7 ps to guarantee

an optimized time domain overlap between the signal and pump pulses to achieve high conversion efficiency. A delay installation composed of collimators and linear translation stage was employed in optical path of the signal to obtain the coincidence between the signal pulses and the pump pulses in time domain.

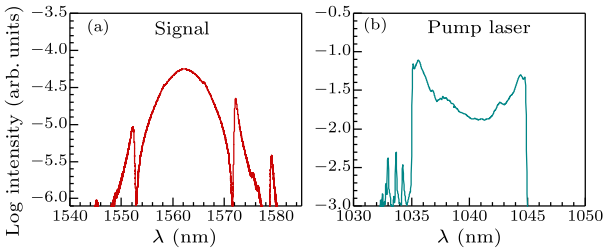

Fig. 2. (a) Spectrum of the signal produced by the EDFL. (b) Spectrum of the amplified pump laser produced by the YDFL and the YDFA.

Both the signal and pump beams were manipulated to be vertical linear polarized by the wave plates and Glan prisms to meet the requirement of type-0 quasi-phase matching in the process of frequency upconversion. A long pass filter cutting off at 1000 nm was inserted in the path of the pump beam to eliminate the stray beams from the LD pump of the YDFL and the YDFA at 980 nm. The infrared signal beam and the pump beam were combined by a dichroic mirror (DM) and focused into the axial center of the MgO:PPLN bulk crystal (HC Photonics Corp.) by an achromatic lens with a focal length of 50 nm. The PPLN bulk crystal was 50 mm-long with a poled period of 11 μm, and the front and rear facades were coated for anti-reflection at 1.04 μm and 1.56 μm. The PPLN crystal was held in a temperature-controlled oven that was fixed on a three-dimensional displacement platform, and the elevation angle and azimuth angle of the oven can be adjusted to make sure that beams propagated parallel to the channel of the PPLN crystal precisely. The operation temperature of the oven as well as the PPLN crystal can be tuned from 20℃ to 200℃ with a fluctuation less than 0.1℃. The SFG beam would generate efficiently when the signal and pump pulses were precisely overlapped spatially and temporally.

A flip mirror (FM) was installed to lead the output beams to different measurement devices. The OSA was employed to monitor the spectrum of SFG and unconverted signal beams with the help of a notch filter centered at 1040 nm to block the intensive pump laser. A collimator was used to couple the SFG beam or the unconverted signal beam into the OSA. The SFG beam can also be sent to a power meter or a Si-APD single-photon counting module (SPCM) to measure the intensity. The SFG beam was steered to pass through a series of spectral filters before arriving at the SPCM or the optical power meter to block the miscellaneous beam from the LD pump laser, the unconverted signal beams, the second harmonic generation of the pump laser and the optical parametric fluorescence induced by the strong nonlinear interaction in the PPLN crystal. The filters include a short-pass filter with a cut-off wavelength at 850 nm, a notch filter at 1040 nm, a pinhole and a bandpass filter with central wavelength at 622 nm and bandwidth of 10 nm. After testing, the total transmittance of the filters and mirrors before SPCM for the SFG photons was 68.0%.

The average power of the signal beam and the pump beam were fixed at 26 μW and 65 mW, respectively. The SFG beam intensities were recorded by a power meter as the temperature of the PPLN was tuned from 85℃ to 185℃ by step of 2℃, the result is depicted in Fig. 3(a). The maximum SFG intensity emerged at the temperature of 116℃, corresponding to a conversion efficiency of 18.6% taking account of the SFG beam transmittance in filters and lens. The curve of the SFG beam intensity showed a flat peak while the PPLN operation temperature changing from 112℃ to 136℃, indicating that the phase matching condition was fulfilled in a broader wavelength range for interacting waves in our upconversion detector (UCD) system. As the temperature tuning from 112℃ to 136℃, most of the signal spectral components address their phase matching pumping partners.

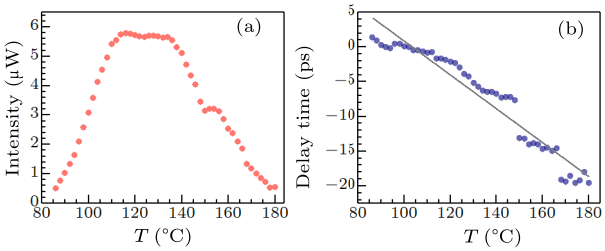

Fig. 3. (a) Intensity of the SFG as a function of temperature of the PPLN crystal when the power of incident signal was 26 μW. (b) Delay time (navy blue balls) between signal pulses and pump pulses under different temperature of the PPLN crystal and fitting line (gray solid line).

For the wide-spectrum signal, the refractive indices at different wavelengths are affected by the temperature of the PPLN crystal to a variable extent, and is the same for the broadband pump. As a result, the relative delay between the signal and the pump should be changed with the temperature to keep the phase velocity of interacting frequency component identical. The relative delay was optimized to achieve the maximum conversion efficiency whenever we changed the temperature of the PPLN crystal. The results were recorded as shown in Fig. 3(b), which shows a linear dependence between the relative delay of beams and the temperature of the PPLN crystal with a fitting slope of −0.24 ps/℃.

We chose the temperature corresponding to the maximum of the signal conversion efficiency to explore the spectrum and bandwidth of converted signal and the SFG. The temperature of the PPLN crystal was set to be 116℃, and the spectrum of the un-

converted signal beam is shown in Fig. 4(a) by gray line with comparison to the original infrared signal beam spectrum shown by the red line. The enclosed area between the incident signal beam spectrum and the unconverted beam spectrum can be considered as the spectral components converted into visible region. The bandwidth of converted signal was about 7.2 nm with the central wavelength at 1562 nm. The SFG was centered at 623 nm with a spectrum linewidth measured to be 0.2 nm as shown in Fig. 4(b). In a comparison of the two spectra before and after frequency conversion, the phase-matching process in the PPLN functioned as a spectrum compressor in the UCD system. The spectrum compression factor from signal to SFG was measured to be 36. According to the spectrum range of the SFG and the converted signal, the spectrum of the pump that participating the frequency conversion process was calculated to be from 1035 nm to 1038 nm with a bandwidth of 3 nm, meaning that not all the pump laser spectral components participated in the SFG. Then the simulated bandwidth of the converted signal was 7.4 nm according to Eq. (5), which is very similar to the experimental result.

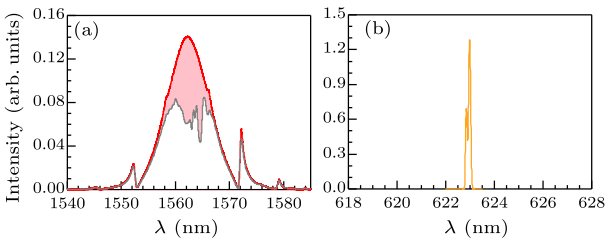

Fig. 4. (a) Spectrum of the signal (solid red line) and unconverted signal (solid gray line). (b) Spectrum of the SFG.

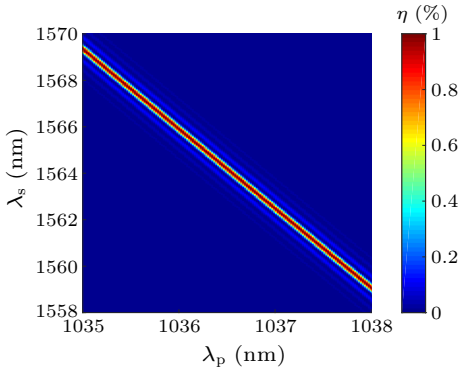

Fig. 5. Simulation of the signal conversion efficiency curve when the signal and pump at different wavelengths linked to the PPLN crystal.

Meanwhile, we have directly simulated the relevance between the wavelengths of the signal and the pump taking part in frequency conversion when the PPLN crystal was at 116℃. We calculated the refractive index of the extraordinary light of the signal and the pump by the Sellmeier equation, and simulated the signal conversion efficiency when the single and the pump was at different wavelengths according to Eqs. (2) and (3), while L was 50 mm and Λ equaled 11 μm, the simulation result is shown in Fig. 5. As can be seen from Fig. 5, the wavelength of the signal has linear relationship with the wavelength of the pump, and the maximum bandwidth that can be converted is about 10 nm when the pump bandwidth is 3 nm. Because of the group velocity mismatch between the signal and the pump, the bandwidth of them is severely restricted.[31] Therefore, only the spectral components from 1035 nm to 1038 nm contributed in the SFG, and the signal spectrum which could participate in this broadband SFG was limited. The group velocity mismatch between the signal and the SFG leads to the compression of the spectral bandwidth.[32]

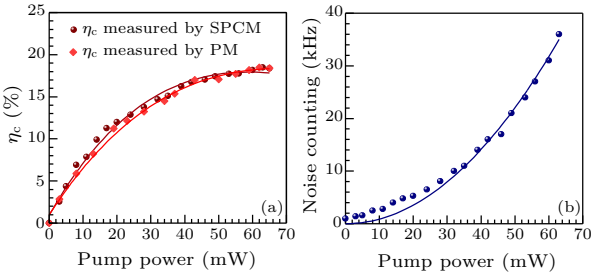

Fig. 6. (a) The curves of conversion efficiency of the signal as a function of the pump power. Wine balls and red diamonds are on behalf of conversion efficiency at different pump power measured by PM and SPCM, respectively, and solid lines are the corresponding fitting curves. (b) The curve of background noise to the pump power. Blue balls show background noise at different pump power when the signal is blocked. Solid blue line is the fitting curve.

The conversion efficiency of broadband signal as a function of the pump power was measured while temperature of the PPLN crystal was fixed at 116℃. When the average power of the signal beam was 26 μW, a power meter was used to evaluate the SFG beam intensity. The conversion efficiency as a function of the pump power was plotted by red diamonds as shown in Fig. 6(a). A maximum conversion efficiency of 18.8% was achieved at a 62 mW pump power. The highest conversion efficiency can be reached notionally to be 18.3%. Even with a perfect overlap of pump and signal beams, conversion efficiency cannot reach 100% because of the Gaussian nature of the beams. Focus effects play probably an important role here as the crystal is long and the focal length of the focusing lens is short. Moreover, temporal fluctuations of the pump and signal due to the multi-longitudinal properties of the lasers play a role in the conversion efficiency so that the total conversion efficiency of the signal was severely limited.

To test the single-photon counting capability of our UCD system, the intensity of the signal beam was attenuated to 8.6×10^{-13} W, corresponding to 0.35 photons per pulse. The specific operation and calculation for the attenuation followed Ref. [15]. Then the measurement was carried out at single-photon level by using the Si-APD single photon counting module (SPCM) (SPCM-AQ-RH-14, Excelitas Technolo-

gies Corp.) to count the SFG photons. The result of measurement is shown in Fig. 6(a) by wine balls. A maximum conversion efficiency of 18.8% was achieved at pump power 63 mW. The fitting curve is shown as the wine line in Fig. 6(a), which is in good agreement with the curve fitted by the data from the power meter measurement.

In conclusion, we have presented a UCD system to convert and detect broadband infrared single photons. By optimizing the spectral bandwidth and pulse durations of pump beam, and accurately controlling the temperature of nonlinear medium to satisfy quasi-phase matching, a maximum conversion efficiency of 18.8% is achieved with a background noise of 1.2×10^{-3} counts/pulse. The spectral bandwidth of the corresponding signal beam participating in the frequency conversion is as broad as 7.2 nm. This scheme of broadband infrared single-photon upconversion and detection provides potential solution in infrared laser ranging, broadband infrared imaging and quantum key distribution.

References

[1] Bennett C H, Brassard G and Mermin N D 1992 *Phys. Rev. Lett.* **68** 557
[2] Bennett C H 1992 *Phys. Rev. Lett.* **68** 3121
[3] Wilk T, Webster S C, Kuhn A and Rempe G 2007 *Science* **317** 488
[4] Chaneliere T, Matsukevich D N, Jenkins S D, Lan S Y, Kennedy T A B and Kuzmich A 2005 *Nature* **438** 833
[5] Kimble H J 2008 *Nature* **453** 1023
[6] Humphreys P C, Kalb N, Morits J P J, Schouten R N, Vermeulen R F, Twitchen D J, Markham M and Hanson R 2018 *Nature* **558** 268
[7] Sun Q C, Mao Y L, Chen S J, Zhang W, Jiang Y F, Zhang Y B, Zhang W J, Miki S, Yamashita T, Terai H, Jiang X, Chen T Y, You L X, Chen X F, Wang Z, Fan J Y, Zhang Q and Pan J W 2016 *Nat. Photon.* **10** 671
[8] Zhang W, Ding D S, Sheng Y B, Zhou L, Shi B S and Guo G C 2017 *Phys. Rev. Lett.* **118** 220501
[9] Liao S K, Cai W Q, Handsteiner J, Liu B, Yin J, Zhang L, Rauch D, Fink M, Ren J G, Liu W Y, Li Y, Shen Q, Cao Y, Li F Z, Wang J F, Huang Y M, Deng L, Xi T, Ma L, Hu T, Li L, Liu N L, Koidl F, Wang P, Chen Y A, Wang X B, Steindorfer M, Kirchner G, Lu C Y, Shu R, Ursin R, Scheidl T, Peng C Z, Wang J Y, Zeilinger A and Pan J W 2018 *Phys. Rev. Lett.* **120** 030501
[10] Mao Y, Wang B X, Zhao C, Wang G, Wang R, Wang H, Zhou F, Nie J, Chen Q, Zhao Y, Zhang Q, Zhang J, Chen T and Pan J 2018 *Opt. Express* **26** 6010
[11] Huo M, Qin J, Cheng J, Yan Z, Qin Z, Su X, Jia X, Xie C and Peng K 2018 *Sci. Adv.* **4** eaas9401
[12] Seri A, Corrielli G, Lago-Rivera D, Lenhard A, Riedmatten H, Osellame R and Mazzera M 2018 *Optica* **5** 934
[13] Lvovsky A I, Sanders B C, Tittel W 2009 *Nat. Photon.* **3** 706
[14] Tanzilli S, Tittel W, Halder M, Alibart O, Baldi P, Gisin N and Zbinden H 2005 *Nature* **437** 116
[15] Ikuta R, Kusaka Y, Kitano T, Kato H, Yamamoto T, Koashi M and Imoto N 2011 *Nat. Commun.* **2** 537
[16] Zhou Z Y, Li Y, Ding D S, Zhang W, Shi S, Shi B S and Guo G C 2016 *Light: Sci. & Appl.* **5** e16019
[17] Pelc J S, Yu L, De Greve K, McMahon P L, Natarajan C M, Esfandyarpour V, Maier S, Schneider C, Kamp M, Höfling S, Hadfield R H, Forchel A, Yamamoto Y and Fejer M M 2012 *Opt. Express* **20** 27510
[18] Dréau A, Tchebotareva A, El Mahdaoui A, Bonato C and Hanson R 2018 *Phys. Rev. A* **9** 064031
[19] Ma J, Chen X, Hu H, Pan H, Wu E and Zeng H 2016 *Opt. Express* **24** 20973
[20] Langrock C, Diamanti E, Roussev R V, Yamamoto Y, Fejer M M and Takesue H 2005 *Opt. Lett.* **30** 1725
[21] Gu X, Huang K, Li Y, Pan H, Wu E and Zeng H 2010 *Appl. Phys. Lett.* **96** 131111
[22] Eisaman M D, Fan J, Migdall A and Polyakov S V 2011 *Rev. Sci. Instrum.* **82** 071101
[23] Markov A, Mazhorova A, Breitenborn H, Bruhacs A, Clerici M, Modotto D, Jedrkiewicz O, Trapani P, Major A, Vidal F and Morandotti R 2018 *Opt. Express* **26** 4448
[24] Choge D K, Chen H X, Xu Y B, Guo L, Li G W and Liang W G 2018 *Appl. Opt.* **57** 5459
[25] Suchowski H, Oron D, Arie A and Silberberg Y 2008 *Phys. Rev. A* **78** 063821
[26] Neely T W, Nugent-Glandorf L, Adler F and Diddams S A 2012 *Opt. Lett.* **37** 4332
[27] Grechin S G, Dmitriev V G, Dyakov V A and Pryalkin V I 2004 *Quantum Electron.* **34** 461
[28] Gagarskiy S, Grechin S, Druzhinin P, Kato K, Kochiev D, Nikolaev P and Umemura N 2018 *Crystals* **8** 386
[29] Lavoie J, Donohue J M, Wright L G, Fedrizzi A and Resch K J 2013 *Nat. Photon.* **7** 363
[30] Jundt D H 1997 *Opt. Lett.* **22** 1553
[31] Allgaier M, Ansari V, Sansoni L, Eigner C, Quiring V, Ricken R, Harder G, Brecht B and Silberhorn C 2017 *Nat. Commun.* **8** 14288
[32] Wabnitz S, Picozzi A, Tonello A, Modotto D and Millot G 2012 *J. Opt. Soc. Am. B* **29** 3128